Materials Science-Poland, 34(1), 2016, pp. 185-191
http://www.materialsscience.pwr.wroc.pl/
DOI: 10.1515/msp-2016-0028

DE GRUYTER OPEN

Structural and electrical properties of chromium substituted nickel ferrite by conventional ceramic method

NUSRAT JAHAN[1], FARUQUE-UZ-ZAMAN CHOWDHURY[1]*, A.K.M. ZAKARIA[2]

[1]Department of Physics, Chittagong University of Engineering and Technology, Chittagong-4349, Bangladesh
[2]Nuclear Safety, Security & Safeguards Division, Bangladesh Atomic Energy Commission, Dhaka, Bangladesh

Polycrystalline Cr substituted Ni ferrites [$NiCr_xFe_{2-x}O_4$ ($0.0 \leqslant x \leqslant 1.0$)] were synthesized by conventional ceramic method and sintered at 1350 °C in air. X-ray diffraction (XRD) patterns showing sharp peaks confirmed the formation of single phase cubic spinel structure. The lattice parameters of the samples were determined from the XRD data using Nelson-Riley extrapolation technique. They were found to decrease with increasing Cr concentration obeying Vegard's law. X-ray density, bulk density and porosity were also calculated from the XRD data. The variation of DC resistivity with temperature was measured by two-probe method. The DC resistivity was found to decrease with increasing temperature indicating the semiconducting nature of the samples. Activation energy was calculated from the Arrhenius plot. AC resistivity, dielectric constant and loss tangent were measured in the frequency range of 1 kHz to 120 MHz at room temperature.

Keywords: *ferrite; XRD; lattice parameter; activation energy; dielectric constant*

1. Introduction

Ferrimagnetic materials are very attractive owing to their potential applications and interesting physical properties. Soft ferrimagnetic oxides with spinel structure find potential applications in electrical components, memory devices, magnetostrictive and microwave devices over a wide range of frequencies because of their high resistivity and low losses [1]. Due to their high resistivity, ferrites are materials of great interest for high frequency inductive components. The applications of ferrites are remarkable due to their good electrical, magnetic and optical properties. AC impedance spectroscopy is a powerful technique to measure the dielectric properties of mixed electronic/ionic conductors. It is an important method to study the electrical properties of ferrites, since the impedance of grains can be separated from other impedance sources, such as impedance of electrodes and grain boundaries. One of the important factors which influences the impedance properties of ferrites is micro-structural effect. Hence, the study of electrical properties is important and useful. The studies on the effect of composition and frequency on the transport properties offer valuable information on the conduction phenomenon as well as the separation of various sources that contribute to the conduction process.

The general chemical formula of spinel ferrite is MFe_2O_4. The compound composed of 32 oxygen anions, 8 cations occupying tetrahedral sites and the rest 16 cations occupying octahedral sites has a close-packed cubic structure with a space group Fd3m [2]. $NiFe_2O_4$ is an inverse spinel ferrite (formula $(Fe^{3+})[Ni^{2+}Fe^{3+}]O_4$) in which tetrahedral sites are occupied by ferric ions and octahedral sites are occupied by ferric and nickel ions [3]. It is suitable as a soft magnetic material in the high frequency region because of its high resistivity and low eddy current loss.

This work is an attempt to prepare and study the structural and electrical properties of $NiCr_xFe_{2-x}O_4$ ferrites by the gradual replacement of Fe^{3+} ions by Cr^{3+} ions. The results of XRD, DC and AC resistivity, activation energy, dielectric

*E-mail: faruque@cuet.ac.bd

constant and loss tangent measurements have been described and discussed.

2. Experimental

Polycrystalline ferrites with the chemical composition $NiCr_xFe_{2-x}O_4$ were synthesized by conventional solid-state ceramic method. Analytical grade Fe_2O_3 (99.00 %), NiO (97.36 %) and Cr_2O_3 (100 %), Sigma-Aldrich, UK, were used as raw materials. Required (stoichiometric) amounts of the chemicals were mixed thoroughly in an agate mortar for 2 h and the mixture was ball-milled for 6 h with ethyl alcohol producing smaller particle size in slurry form. The slurry in a form of a mixture was dried until it turned into powder. After homogeneous mixing of the sample in the ball-mill, the slurry was dried by a magnetic heater until it became a loose powder. The mixture was milled again for 1 h. The fine dry powder was pre-sintered at 1000 °C for 8 h and then cooled slowly in a furnace. After calcining, the mixture was again milled for 1 h to obtain a homogeneous material. After pre-sintering the sample was again ground into fine powder in the agate mortar. The fine powder was mixed with a small amount of polyvinyl alcohol as a binder and the powder was pressed (15 kN/m^2) into compacts of desired shapes.

At last sintering was performed using a programmable furnace NABER (HTCT 08/16) at 1350 °C for 8 h with the temperature ramp of 5 °C/min for heating and 6 °C/min for cooling.

X-ray diffraction study was carried out in order to check the phase purity and to perform structural analysis using a Philips X'Pert PRO X-ray diffractometer with CuKα radiation ($\lambda = 1.5418$ Å). The diffraction data were recorded between 15° to 65° in steps of 0.02°. The database used for the analysis of the diffraction data was X'Pert Highscore. DC resistivity was measured at room temperature by two probe method using Keithley 6514. AC electrical properties were measured using an impedance analyzer (Wayne Kerr 6500B) at room temperature up to 120 MHz.

3. Results and discussion

3.1. Structural study

Fig. 1 shows the X-ray diffraction patterns of $NiCr_xFe_{2-x}O_4$ ferrites sintered at 1350 °C. The peaks can be indexed to (1 1 1), (2 2 0), (3 1 1), (2 2 2), (4 0 0), (4 2 2), (5 1 1) and (4 4 0) planes. The samples can be identified as a single-phase cubic spinel structure with no extra lines corresponding to any other crystallographic phase. The sharp peaks in the XRD patterns confirmed the formation of a homogeneous single phase cubic spinel structure corresponding to the space group Fd3m for all the samples. The lattice parameters were calculated from the XRD data.

The lattice constant "a" of each sample was calculated using the relation:

$$a = d(h^2 + k^2 + l^2)^{1/2} \tag{1}$$

where d = interplanar distance and (h k l) are the Miller indices.

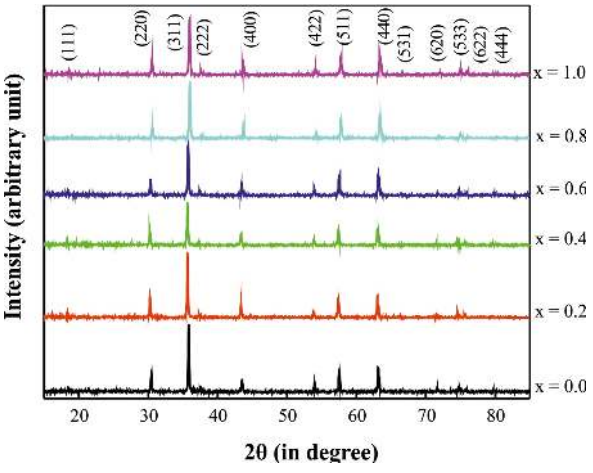

Fig. 1. X-ray diffraction pattern for the $NiCr_xFe_{2-x}O_4$ system sintered at 1350 °C.

The variation of lattice constant with Cr concentration is shown in Fig. 2. It is observed that as the Cr content increases the lattice parameter decreases. This variation of lattice parameter can be explained by the difference of ionic radii between Cr^{3+} and Fe^{3+}. The ionic radius of Cr^{3+} (0.64 Å) is relatively smaller than that of Fe^{3+} (0.67 Å) [2]. As there occurs a partial replacement of Fe^{3+} in

the octahedral sites by Cr^{3+}, the shrinkage of lattice parameter happens. It can also be explained by the migration of cations. The linear variation of lattice parameters with Cr concentration confirms the applicability of Vegard's law.

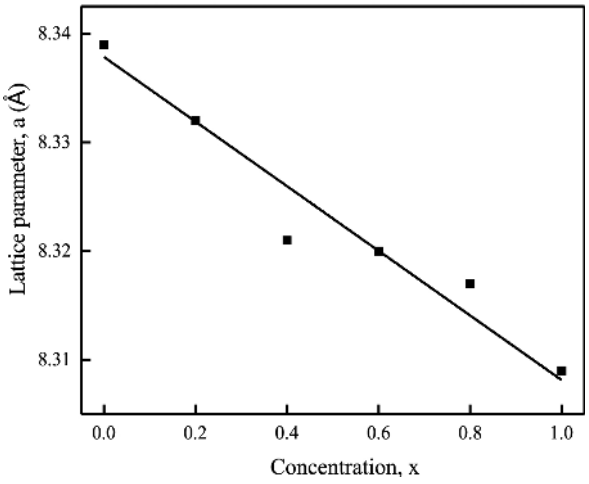

Fig. 2. Variation of lattice parameters with the concentration of Cr for the $NiCr_xFe_{2-x}O_4$ system sintered at 1350 °C.

The X-ray density ($\rho_x = 8$ M/Na^3, where M is the molecular weight of the corresponding composition and N is Avogadro's number) and the bulk density (ρ_b = m/V, where $V = a^3$ is the volume of the cubic unit cell) were calculated using the lattice parameter "a" obtained from the XRD measurements.

Both the bulk density and the X-ray density decrease with the increase in Cr concentration. This is due to the smaller molar mass of the Cr (51.996 g/mol) cation substituted in place of Fe with larger molar mass (55.845 g/mol) [4]. It is observed that the bulk density is lower than the X-ray density. This is due to the existence of pores which arise during the preparation and/or the sintering process of the samples. As porosity is inversely related to the density, in general, the values of porosity increase with the increase in Cr addition.

The porosity was calculated from the bulk density and X-ray density using the formula:

$$P = (1 - \rho_b/\rho_x) \times 100\,\% \qquad (2)$$

The calculated lattice parameter, bulk density, X-ray density and porosity are presented in Table 1.

3.2. DC resistivity

Resistivity depends on the microstructure of ferrite. With increasing porosity, resistivity also increases, since pores do not take part in conduction [4]. Substitution of Cr^{3+} in place of Fe^{3+} increases the DC electrical resistivity as a result of the formation of stable electric bonds between the Cr^{3+} and Fe^{2+}, placing Fe^{2+} charge carriers in localized states. The decrease in Fe^{3+} ion content leads to the decrease of ferrous ions formed. This leads to the migration of some Fe^{3+} ions from B sites to A sites, and as a result, the number of Fe^{3+} and Fe^{2+} ions at the B sites decreases. The increase in Cr^{3+} content leads to replacement of Fe^{3+} ions at B sites. Consequently, the resistivity increases on increasing substitution of Cr^{3+} ions [5].

DC electrical resistivity has been measured in air as a function of temperature between room temperature and 450 °C. Each sample was polished and silver paste was applied on both sides of the polished pellet together with two thin copper wires. Fig. 3 depicts that DC resistivity decrease with increasing temperature which means that the conductivity increases. The decrease in resistivity is attributable to the increase in the drift mobility of electric charge carriers due to enhanced oscillation of crystal lattice. This decrease in resitivity indicates the semiconductor nature of all the samples. In polycrystalline ferrites, the bulk resistivity is the combination of crystalline resistivity and the resistivity of the crystalline boundaries. Boundary resistivity is greater than the crystalline resistivity. Consequently, the boundary resistivity has a great influence on the bulk resistivity [6]. An increasing tendency in DC resistivity is observed with increasing Cr concentration [7].

3.3. Activation energy

In ferrites, the resistivity (ρ) at absolute temperature (T) is represented by the relation:

$$\rho = \rho_0 \exp(\Delta E/kT) \qquad (3)$$

Table 1. Lattice parameter, X-ray density, bulk density, porosity and activation energy for $NiCr_xFe_{2-x}O_4$ sintered at 1350 °C.

Concentration	Lattice parameter	X-ray density	Bulk density	Porosity	Activation energy [eV]		
x	a [Å]	ρ_x [g/cm^3]	ρ_b [g/cm^3]	P [%]	E_f	E_p	$\Delta E = E_p - E_f$
0.0	8.339	5.452	4.515	17.20	0.14	1.74	1.60
0.2	8.332	5.445	4.577	15.94	0.13	2.31	2.18
0.4	8.321	5.445	4.398	19.23	0.10	1.94	1.84
0.6	8.320	5.425	4.272	21.26	0.34	0.96	0.62
0.8	8.317	5.410	4.284	20.81	0.40	1.03	0.63
1.0	8.309	5.404	4.090	24.32	0.36	1.19	0.83

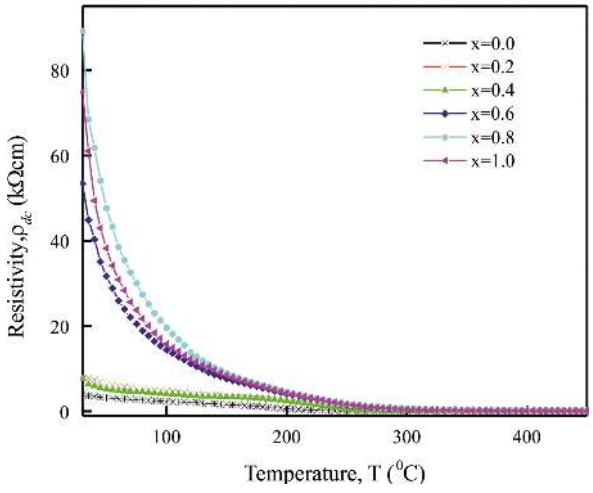

Fig. 3. Variation of DC resistivity with temperature for the $NiCr_xFe_{2-x}O_4$ system sintered at 1350 °C.

where k is the Boltzmann constant and ΔE is the difference between the activation energies in ferromagnetic (E_f) and paramagnetic (E_p) regions. The activation energy is required to release an electron from Fe^{2+} to the neighboring ion. These extra electrons can contribute the electrical current by jumping or hopping process. According to the Verwey model, the electrical conduction in ferrite can take place by exchanging electrons among the octahedral ions (hopping mechanism) [8–12]. The normal distance between tetrahedral-tetrahedral or tetrahedral-octahedral is large in comparison to octahedral-octahedral so that the electronic exchange between the cations on these sites is low.

The variation of resistivity against inverse of temperature of the samples is shown in Fig. 4. The slope in the low temperature region is regarded as ferromagnetic and it changes into paramagnetic in high temperature region. Activation energy is attributed to a change in conduction mechanism or phase transition from ferromagnetic to paramagnetic. The curves show that the slope changes with temperature which indicates that the activation energy changes with temperature too. The temperature at which the slope is changed does not match the Curie temperature of the respective sample [10]. From the slope (Fig. 4), ΔE (presented in Table 1) was calculated using the formula [11]:

$$\Delta E = slope \times 4.606 \times 8.62 \times 10^{-5}\ \text{eV} \qquad (4)$$

The activation energy in ferromagnetic region is smaller than in the paramagnetic region. In the ferromagnetic region, the activation energy is caused by electron hopping through a single-charged oxygen vacancy and it is attributed to the magnetic spin disordering due to decrease in the concentration of current carriers [11–14]. In the paramagnetic region, the activation energy is above 0.5 eV, which is much larger than the ionization energy for donor or acceptor or for Fe^{2+}–Fe^{3+} transition energy. Therefore, the band type conduction is not possible and conduction is due to hopping of polaron [15]. The general trend of the value of the activation energy (ΔE) is to decrease with the increase of Cr concentration.

3.4. AC resistivity

The variation of AC resistivity with frequency at room temperature is shown in Fig. 5. For all the samples, it is observed that as frequency increases

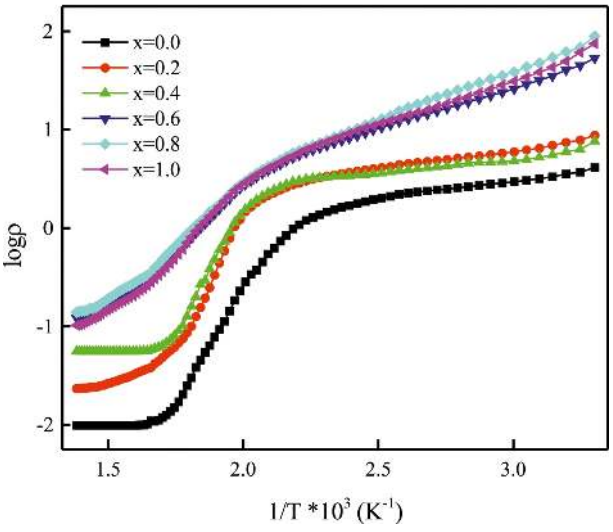

Fig. 4. logρ vs. 1/T curve of the $NiCr_xFe_{2-x}O_4$ system sintered at 1350 °C for measuring the activation energy.

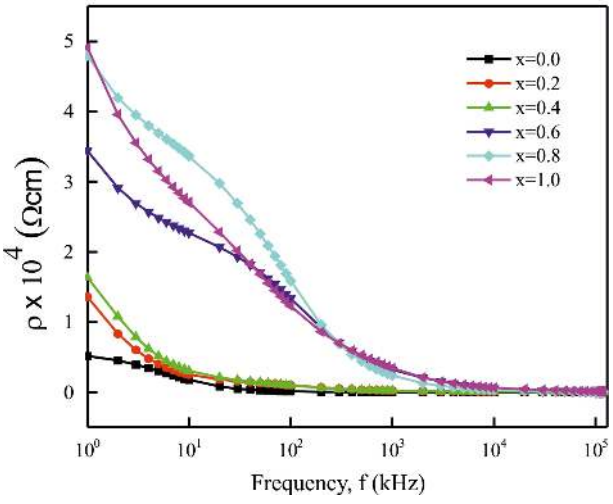

Fig. 5. Variation in AC resistivity with frequency for all the samples of the $NiCr_xFe_{2-x}O_4$ system sintered at 1350 °C.

the resistivity decreases. The dispersion of AC resistivity in low frequency region is large and above 10 MHz it remains constant up to frequency of 120 MHz. This dispersion of resistivity can be explained on the basis of Koop's phenomenological theory. AC resistivity decreases as the frequency increases since at high frequency polarization of the dipoles decreases [2].

Above a certain frequency, the electron exchange does not follow the applied alternating field. The increase in frequency enhances the hopping frequency of the charge carriers between Fe^{2+} and Fe^{3+} ions. These enhanced electrons increase the conduction and thereby decrease the resistivity [16]. The AC resistivity is found to increase with the increase in Cr concentration in the low frequency region.

3.5. Dielectric constant (ε') and dielectric loss (tanδ)

The real part of dielectric constant was calculated from the formula:

$$\varepsilon' = \frac{CL}{\varepsilon_o A} \tag{5}$$

where C is the capacitance in pF, L is the thickness or height of the pellet, A is the cross-sectional area of the circular surface of the pellet and $\varepsilon_o = 8.854 \times 10^{-14}$ F/cm is the free space permittivity. Fig. 6 shows the dependence of ε' on frequency. From these curves it is evident that as the frequency increases, the dielectric constant decreases. The dielectric constant is dependent on frequency in the lower frequency region and independent in the higher frequency region. At higher frequency these values are almost constant. When the electric field propagates with high frequency, the ionic and orientation sources of polarization of the dipoles decrease and beyond a certain frequency electron exchange does not follow the alternating field, which results in a constant value of dielectric constant. This behavior is attributed to the Maxwell-Wagner type space charge polarization which agrees with the Koop's phenomenological theory [17]. The decrease of ε' with Cr content resulted in a decrease of dielectric loss [18]. At lower frequency the high value of ε' is due to the predominance of the species, such as Fe^{2+} ions, oxygen vacancies, grain boundary defects, interfacial distribution, etc. During the sintering process, electron exchange occurs between $Fe^{2+} \leftrightarrow Fe^{3+}$ which leads the displacement of electron in the direction of applied field that determines the polarization [19].

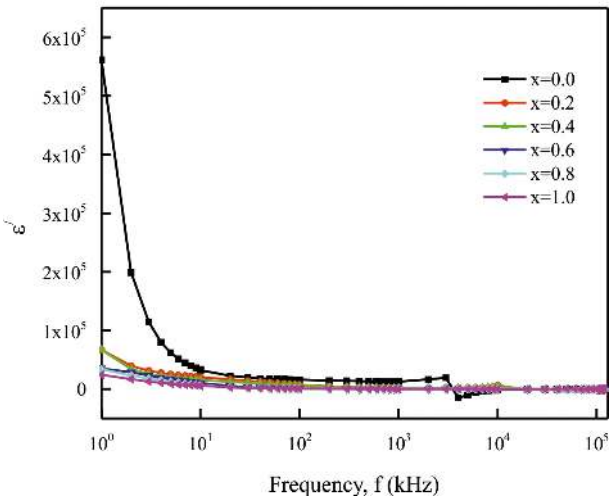

Fig. 6. Variation of dielectric constant with frequency of the $NiCr_xFe_{2-x}O_4$ system sintered at 1350 °C.

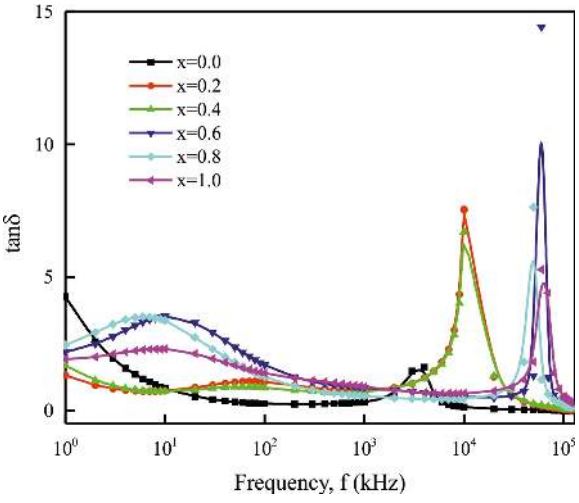

Fig. 7. Variation of loss tangent with frequency for the $NiCr_xFe_{2-x}O_4$ system sintered at 1350 °C.

In polycrystalline ferrites, the dielectric loss tangent is the result of energy dissipation in a dielectric which is due to the lagging of polarization with respect to the applied alternating field. Fig. 7 depicts the dielectric loss behavior of the $NiCr_xFe_{2-x}O_4$ system which shows asymmetrical behavior. In this figure, there is a peak in the power loss owing to the transfer of the maximum electrical energy to the oscillating ions when the frequency of the external AC field is equal to the hopping frequency of the charge carriers [20]. The occurrence of the loss peak in the tanδ versus frequency is associated with the correlation between the hopping conduction mechanism and dielectric behavior of spinel ferrites.

4. Conclusions

Polycrystalline $NiCr_xFe_{2-x}O_4$ ($0.0 \leqslant x \leqslant 1.0$) ferrites were prepared by conventional ceramic technique. The ferrite samples possess a single phase cubic spinel structure. Both the X-ray and bulk densities decrease with Cr content, whereas the porosity increases. The hopping type conduction mechanism is typical of these materials. The conduction mechanism has been confirmed by the values of activation energy. The AC resistivity decreases with frequency. The higher frequency enhances the hopping of charge carriers between the Fe^{2+} and Fe^{3+} ions, and as a result the conduction increases and resistivity decreases. The dielectric constant decreases with frequency up to 10 MHz and then it takes a constant value. The loss peak is related to the hopping conduction mechanism and dielectric behavior.

Acknowledgements

We are thankful for the laboratory support of the Institute of Nuclear Science & Technology and the Materials Science Division, Atomic Energy Commission, Dhaka, Bangladesh. The authors are grateful to the authority of the Chittagong University of Engineering and Technology, Chittagong-4349, Bangladesh, for the financial assistance of the research work.

References

[1] MUND H.S., SHAILJA T., JAGRATI S., ITOU M., SAKURAI Y., AHUJA B.L., *J. Appl. Phys.*, 110 (2011), 073914.

[2] HASHIM M., MEENA S.S., KOTNALA R.K., SHRSATH S.E., ROY A.S. PARVEEN A., BHATT P., KUMAR S., JOTANIA R.B., KUMAR R., ALIMUDDIN, *J. Alloy. Compd.*, 602 (2014), 150.

[3] DIXIT G., SINGH J.P., SRIVASTAVA R.C., AGRAWAL H.M., CHAUDHARY R.J., *Adv. Mater. Lett.*, 3 (2012), 21.

[4] ELHITI M.A., *J. Magn. Magn. Mater.*, 136 (1994), 138.

[5] KRISHNA K.R., KUMAR K.V., RAVINDER D., *Adv. Mater. Phys. Chem.*, 2 (2012), 185.

[6] NARAYAN R., TRIPATRI R.B., DAS B.K., *Proceedings of the Fifth International Conference on Ferrite. Bombay, India*, (1989), 267.

[7] KITTEL C., *Introduction to Solid State Physics*, John Wiley & Sons Inc. New York, 1976.
[8] VERWEY E.J.W., DE BOER J.H., *Recueil des Travaux Chimiques des Pays-Bas*, 55 (1936), 531.
[9] LAISHRAM R., PHANJOUBAM S., SARMA H.N.K., PRAKSH C., *J. Phys. D-Appl. Phys.*, 32 (1999), 2151.
[10] BAIJAL J.S., PHANJOUBAM S., KOTHARI D., PRAKASH C., KISHAN P., *Solid State Commun.*, 83 (1992), 679.
[11] CHAUDHURI S.P., SARKAR P., CHAKRABORTY A.K., *Ceram. Int.*, 25 (1999), 91.
[12] BRACHWITZ K., BONTGEN T., LORENZ M., GRUNDMANN M., *Appl. Phys. Lett.*, 102 (2013), 172104.
[13] BÄRNER K., MANDAL P., HELMOLT R.V., *Phys. Status Solidi B*, 223 (2001), 811.
[14] SHITRE A.R., KAWADE V.B., BICHILE G.K., JADHAV K.M., *Mater. Lett.*, 56 (2002), 188.
[15] PATIL A.N., MAHAJAN R.P., PATANKAR K.K., GHATAGE A.K., MATHE V.L., PATIL S.A., *Indian J. Pure Ap. Phy.*, 38 (2000), 651.
[16] BACHHAV S.G., PATIL A.A., PATIL D.R., *Adv. Ceram. Sci. Eng.*, 2 (2013), 89.
[17] KOOP C.G., *Phys. Rev.*, 83 (1951), 121.
[18] NASIR S., ANIS-UR-REHMAN M., MALIK M.A., *Phys. Scripta*, 83 (2011), 025602.
[19] BATOO K.M., *Physica B*, 406 (2011), 382.
[20] SIVAKUMAR N., NARAYANASAMY A., JEYADEVAN B., JOSEYPHUS R.J., *J. Phys. D-Appl. Phys.*, 41 (2008), 245001.

Received 2015-12-02
Accepted 2016-01-05